Environmental Pollution 311 (2022) 119909

Contents lists available at ScienceDirect

Environmental Pollution

journal homepage: www.elsevier.com/locate/envpol

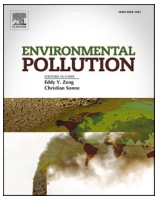

Enhanced settling of microplastics after biofilm development: A laboratory column study mimicking wastewater clarifiers☆

So-Young Lee, Jiyul An, Jinwoo Kim, Jung-Hwan Kwon *

Division of Environmental Science and Ecological Engineering, Korea University, 145 Anam-ro, Seongbuk-gu, Seoul, 02841, Republic of Korea

ARTICLE INFO

Keywords:
Microplastics
Settling velocity
Biofilm
Aggregation
Wastewater treatment plants
Freshwater

ABSTRACT

The settling of microplastics (MPs) is crucial for their removal from municipal wastewater treatment plants (WWTPs) and sedimentation in static waterbodies, where they can accumulate in bottom sediments. Biofilm formation on MPs enhances their aggregation with other particles, thereby changing their density and size and altering their settling rates. However, only a few studies have investigated the settling of MPs of different sizes and materials. Specifically, the settling of small-sized MPs (<150 μm) has been poorly documented. In this study, cylindrical and fragmented particles of four polymer types (high-density polyethylene (HDPE), polypropylene (PP), polystyrene (PS), and poly(ethylene terephthalate) (PET)) were used to investigate the settling or floating of reference MPs (20–130 μm) in a custom-made column that simulated a primary sedimentation tank in a typical WWTP before and after incubation in wastewater influent. The settling velocity of the reference MP particles was strongly influenced by the particle size and density. The settled fractions of all the cylindrical reference MPs increased significantly (up to 5 times) due to biofilm formation at overflow velocities of 0.15, 0.26, and 0.40 mm s^{-1}. This was observed even for HDPE and PP (density <1 g cm^{-3}) after biofilm formation. The fragmented reference MPs showed complex and rather unpredictable behavior, possibly due to their irregular shape. Generally, the settling of pristine PS and PET in the laboratory tests was consistent with the theoretical predictions obtained using Stokes' law. The experimental findings of this study can be used to develop models that predict the removal efficiencies of MPs in WWTPs and to estimate the sinking of MPs to bottom sediments of static waterbodies.

1. Introduction

The extensive and widespread use of plastics has resulted in plastic pollution. There has been a steady rise in the production of plastics globally, with more than 367 million tons in 2020 (Plastics Europe & EPRO, 2021). The COVID-19 pandemic has led to an increase in the consumption of single-use plastic-based personal protective equipment, further increasing plastic pollution (Adyel, 2020). Inappropriate disposal of plastic products leads to their degradation and fragmentation in the environment, thereby generating small debris.

Microplastics (MPs) are plastic particles that range between 0.1 μm and 5 mm in size (ATC, 2021). They have been documented in oceans (Andrady, 2005; Cózar et al., 2014; Thompson, 2004), terrestrial systems (Wong et al., 2020), and freshwater systems (Baldwin et al., 2016; Free et al., 2014; Lahens et al., 2018; McCormick et al., 2014; Rochman, 2018). In 2016, approximately 19–23 Mt, or 11%, of plastic waste was found in aquatic ecosystems, including rivers, lakes, and oceans. If this trend continues, this number could reach 90 Mt/year by 2030 (Borrelle et al., 2020). However, the amount of plastic debris on the ocean surface accounts for only approximately 1% of the projected waste input from land (Cózar et al., 2014; Law and Thompson, 2014; van Sebille et al., 2015), indicating a large difference between the sources and sinks of MPs. One possible hypothesis explaining the missing load of MPs in oceans is the sedimentation or settling of MPs in freshwater systems and oceans. This hypothesis is partly supported by the fact that the estimated annual river emissions into oceans globally (0.8–2.7 Mt/year) (Meijer et al., 2021) were found to be lower than plastic inputs into the entire aquatic system studied (Borrelle et al., 2020). MPs generated on land can

Abbreviations: C_D, drag coefficient; FT-IR, Fourier-transform infrared spectroscope; HDPE, high-density polyethylene; MP, microplastic; PE, polyethylene; PET, poly(ethylene terephthalate); PP, polypropylene; PS, polystyrene; *Re*, Reynolds number; SEM, scanning electron microscopy; WWTP, wastewater treatment plant.

☆ This paper has been recommended for acceptance by Eddy Y. Zeng.

* Corresponding author.
E-mail address: junghwankwon@korea.ac.kr (J.-H. Kwon).

https://doi.org/10.1016/j.envpol.2022.119909
Received 14 May 2022; Received in revised form 21 July 2022; Accepted 3 August 2022
Available online 12 August 2022

be retained in freshwater systems for long periods, until they reach oceans (Alimi et al., 2018). Several studies have explored the distribution and fate of MPs in freshwater systems. They have revealed that static waterbodies, such as lakes, ponds, and reservoirs, could be potential regions of MP accumulation (Di and Wang, 2018; Hu et al., 2018; Sruthy and Ramasamy, 2017; Welden and Lusher, 2020). High concentrations of MPs in river and lake sediments indicate the retention of MPs in freshwater systems.

Although typical municipal wastewater treatment plants (WWTPs) remove MPs with an overall efficiency of >90% (Iyare et al., 2020; Park et al., 2020; Sol et al., 2020; Tang and Hadibarata, 2021), WWTPs continue to be the major point sources of MPs (Hu et al., 2022). The most important removal mechanism of MPs in WWTPs is particle settling in clarifiers after coagulation with other particles, with removal efficiencies of 53–92% (Carr et al., 2016; Dris et al., 2015; Gies et al., 2018; Long et al., 2022; Talvitie et al., 2015; Yang et al., 2019). However, the removal of MP particles from individual polymers by settling has been poorly documented, and only large MPs (598–1618 μm) have been studied (Murphy et al., 2016). Size of MPs in WWTP effluents were smaller than those in the influents, suggesting a more efficient removal of larger MPs in WWTPs (Dris et al., 2015; Simon et al., 2018; Talvitie et al., 2017). Due to the experimental difficulties associated with smaller particles, it is still unclear how relatively smaller MPs (<~150 μm) are removed (Iyare et al., 2020; Sol et al., 2020). As smaller MPs are suspected to exert more severe effects on aquatic organisms (An et al., 2021; Bhagat et al., 2021; Ge et al., 2021; Kokalj et al., 2018; Ma et al., 2020; Ziajahromi et al., 2018), understanding their settling in typical WWTPs is important for assessing the loading of MPs into freshwater and their potential adverse effects on aquatic environments.

The settling behavior of MPs is not only influenced by the hydraulic conditions of waterbodies but also by the characteristics of the MPs. In static water with a small Reynolds number, the settling rate is determined by the density, size, and shape of an MP particle (Stokes, 1851). High-density MPs are readily deposited into lakes and reservoirs in the form of bottom sediment (Di and Wang, 2018; Xiong et al., 2018). It was found that polyethylene (PE), polypropylene (PP), and poly(ethylene terephthalate) (PET) were the most prevalent MPs in water and sediments because they are produced and used in large quantities. However, a relatively high proportion of MPs with densities higher than that of water, such as polystyrene (PS), polycarbonate, polyvinylchloride, and nylon, was also detected in sediment samples. These results were supported by laboratory studies that investigated the terminal velocities of pristine MPs with regular or irregular shapes, which demonstrated that the settling of MPs is well described by the Stokes equation (Khatmullina and Isachenko, 2017; Waldschläger and Schüttrumpf, 2019). Generally, the size of reference MPs used in settling experiments is larger than 0.5 mm, although MPs isolated from water and sediment samples are generally much smaller (Di and Wang, 2018; Fischer et al., 2016; Free et al., 2014; Su et al., 2016; Xiong et al., 2018). As particulate behavior in water depends mainly on the particulate size, it is necessary to understand the settling behavior of MPs with small size ranges.

Biofouling allows the aggregation of MPs with suspended particles, which increases their density and allows MPs with lower densities to settle in waterbodies (Horton et al., 2017). Higher proportions of PE and PP, which have densities lower than that of water, have been detected in the sediment of lakes, reservoirs, and rivers (Di and Wang, 2018; Eo et al., 2019; Koutnik et al., 2021; Xiong et al., 2018). MPs provide surfaces for the colonization of microbial communities and formation of biofilms (Miao et al., 2019), which alter their properties and play an important role in the heterogeneous aggregation of MPs. For example, Michels et al. (2018) observed accelerated aggregation of PS beads (700–900 μm) with other biogenic particles in seawater after biofilm formation. In addition, Semcesen and Wells (2021) demonstrated that the increasing velocities for irregularly shaped PP granules (approximately 125–2,000 μm) decreased in *ex situ* column experiments as the formation of biofilm progressed. Moreover, some PP particles covered with biofilm were observed to settle. Similar to settling experiments with pristine MPs, this study used relatively larger PP particles. Further research on diverse MP materials with small sizes (<150 μm) is required because biofilm formation, aggregation, and the settling of MPs depend on their physical and chemical characteristics.

The aims of this study were to (1) quantitatively investigate the settling or floating of small MPs (<150 μm) in WWTP influents in a vertical flow system that simulates the primary sedimentation tank in WWTPs and (2) evaluate the effects of biofilm formation on the settling of MPs. For the settling experiment, four types of polymers (high-density polyethylene (HDPE), PP, PET, and PS) were selected because of their abundance in freshwater systems (Koutnik et al., 2021) and effluents of WWTPs (Simon et al., 2018; Talvitie et al., 2017; Yang et al., 2019). Small MPs (<150 μm), which are dominant in the environment, including in WWTP influent, but have rarely been investigated for their settling behavior, were the target MPs in this study. Cylindrical reference MPs (diameter: 80–130 μm, length: approximately 100 μm) of the four plastic materials and fragmented reference PS and PET sieved through a 20–100-μm mesh were used. These reference MPs were incubated in the WWTP influent to allow biofilm formation, after which settling experiments were conducted at three overflow velocities. The settled fraction was evaluated for all reference MPs before and after incubation, and the results were compared with theoretical predictions.

2. Materials and methods

2.1. Materials

HDPE, PP, and PS pellets were purchased from LG Chem Ltd. (Seoul, Republic of Korea), and PET pellets were purchased from Lotte Chemical (Seoul, Republic of Korea). Custom-made reference MPs of PS and PET (size: 20–100 μm) were generously supplied by the Korea Testing & Research Institute (KTR) (Gwacheon, Gyeonggi-do, Korea). Sodium iodide (NaI, 99.5% purity) was purchased from FUJIFILM Wako Pure Chemical Corporation (Osaka, Japan).

2.2. Preparation and characterization of reference MP particles

To prepare the reference cylindrical MP particles, pellets of the four polymers were molded into fibers with 80–130 μm diameters using a plastic extruder (LME-230, Dynisco, Franklin, MA). The fibers were cut to a length of approximately 100 μm using a microtome (Microm HM200; Microm International, Walldorf, Germany). The cross-sectional diameter and length of the cylindrical reference MP particles were measured from images captured using a BX51 microscope coupled with a DP20 camera (Olympus, Tokyo, Japan). Image analysis was performed using the IMAGEJ software 1.53a (National Institutes of Health, Bethesda, MD, USA). The density of the reference MP particles for each polymer material was measured using a modified titration method (Beuth, 2013) with 99% ethanol, distilled water, and an NaI solution (density: 1.58–1.60 g mL^{-1}). The densities of the HDPE and PP were determined by gradually adding distilled water into 99% ethanol containing standard MPs until the MPs floated to the surface of the solution and measuring the volume and mass of the added solution. The densities of the HDPE and PP were 0.956 g cm^{-3} and 0.889 g cm^{-3}, respectively. For PS and PET, the NaI solution and ethanol were used. The measured densities of the cylindrical PS and PET were 1.053 and 1.327 g cm^{-3}, respectively. The reference MP particles provided by the KTR were fragmented particles with irregular shapes, and their sizes and densities were measured using the same methods before the tests. The measured densities of the fragmented PS and PET were 1.049 g cm^{-3} and 1.358 g cm^{-3}, respectively.

2.3. Biofilm development on MPs in WWTP influent solution

For this experiment, influent wastewater was collected from the

Jungnang Sewage Treatment Plant (Seoul, Republic of Korea) on September 4, 2021, using grab sampling. A stainless-steel bucket was submerged into the WWTP influent reservoir at a depth of 0.4–0.5 m, and the collected sample was poured into two 20 L PE square bottles. The samples were transferred to a laboratory and stored at 4 °C until further use.

For the formation of biofilms at the surface of the MPs, reference MPs were incubated in the collected influent solution. Approximately 100–150 reference MP particles were counted under an optical microscope and added to a 50 mL conical tube containing 20 mL of wastewater influent. The tubes were incubated at 25 °C, illuminated by light-emitting diode (LED) lamps (approximately 3,000 lx), and shaken using a digital rotary shaker (60 rpm) for two weeks. Although the hydraulic retention time of sewage water in WWTPs is generally less than two days (Deowan et al., 2015; Karabelas et al., 2018), aged MPs covered by fully developed biofilms are likely to enter WWTPs. Therefore, two weeks was chosen as the incubation duration to allow sufficient formation of biofilms on the pristine reference MPs. The LED lamps and light/dark periods (12:12 h) adopted in this study were chosen as the typical culturing conditions for microalgae in the freshwater (Kang et al., 2016; OECD, 2011).

2.4. Vertical transport of MPs in WWTP influent solution

Column studies were conducted in series to evaluate the settling velocity of the reference MP particles before and after incubation in the WWTP influent solution. The collected WWTP influent was filtered through a stainless-steel filter (dimeter: 25 mm, pore size: and 20 μm) to prevent clogging of the test system by other suspended particles in the influent. A schematic diagram of the custom-made vertical-transport test apparatus is shown in Fig. 1. The influent solution was placed at the bottom of a settling glass column (height: 45 cm, inner diameter: 52 mm) using a peristaltic pump (BT100-1F, Baoding Longer Precision Pump Co., Ltd, Hebei, China) with Tygon® crystal clear laboratory tubing (id/od 4.8/7.9 mm). The overflow from the settling column was collected in an aluminum duct and directed to the influent reservoir for recirculation before injecting the reference MPs. After setting the flow rate by measuring the overflow rate, the three-bed volumes of the influent were recirculated to stabilize the test apparatus. After stabilization, the reference pristine or incubated MP particles were injected at the bottom of the settling cylinder using a 30 mL glass syringe equipped with a 50 cm-long stainless-steel pipe (internal diameter: 4.2 mm). After injecting the MP particles, the aluminum duct was disconnected from the influent reservoir, and approximately 800–1000 mL of the column overflow was filtered through a 25-mm stainless-steel filter (pore size: 20 μm for the cylindrical MP particles and 5 μm for the smaller fragmented MP particles) to collect sufficient MP particles. Furthermore, the settling column was disconnected from the peristaltic pump, and the remaining WWTP influent in the column was drained. MP particles in the first 200 mL of drainage were considered settled particles, whereas the remaining MP particles were considered suspended particles. The drainage was also filtered through a 25-mm stainless-steel filter (pore size: 20 μm). The tested flow rates were set to approximately 10, 25, and 35 mL min^{-1}. Moreover, the actual flow rates were calculated based on the measured volume of the overflow. All settling experiments were conducted twice.

2.5. Pretreatment of samples

MP particles collected on stainless-steel filters were retrieved and pretreated before spectroscopic identification using a Fourier-transform infrared spectroscope (FT-IR) with a dissection microscope (Nicolet iN10 MX, Thermo Fisher Scientific, Waltham, MA). A stainless-steel filter was submerged in a 20 mL glass vial containing 5 mL of distilled water. The vial was sonicated for 30 min to detach the particles from the filters. After sonication, the filter was picked up and rinsed with 4 mL distilled water and 9 mL of 30% hydrogen peroxide to remove any remaining particles. Thereafter, the rinsate was added to the pretreatment vial. The vial was placed in a dry oven at 60 °C for 3 h, allowing wet peroxidation with hydrogen peroxide. The oven temperature was then increased to 85 °C to evaporate the solution. After the solution had completely evaporated, the vial was removed from the oven. For density

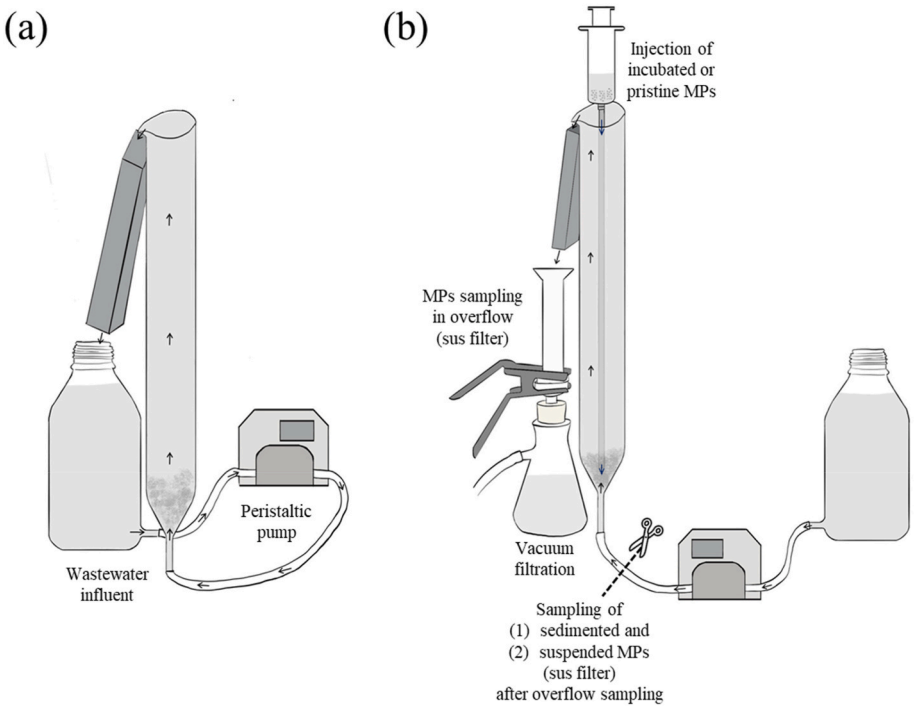

Fig. 1. Schematic diagram of the vertical-transport test system for measuring the settling of MPs in WWTP (a) during stabilization before injecting reference MPs and (b) during the settling experiment after injecting reference MPs.

separation of the MP particles, 20 mL of an NaI solution (1.6 g mL^{-1}; filtered through a Whatman grade GF/C glass microfiber filter with a pore size of 1.2 μm) was added to the glass vial, which was placed in a glass cup. The MPs were allowed to float near the surface for 3 h, after which the NaI solution was carefully added to the vial to allow the floating MPs to overflow. The surface of the vial was rinsed in a glass cup using the NaI solution and then the solution in the cup was filtered through a 25-mm Whatman Anodisc inorganic filter membrane with a pore size of 0.2 μm. The Anodisc filters were secured in a clean glass Petri dish and dried in a vacuum desiccator.

2.6. Spectroscopic determination of reference MPs

The particles collected on the Anodisc filter were analyzed using the FT-IR instrument. The spectrum of each pure reference MP material was obtained at a collection time of 0.314 s and resolution of 4 cm^{-1}; this was the reference spectrum (Fig. S1). The spectra of the entire area of the filters were obtained by scanning at a collection time of 0.314 s, resolution of 16 cm^{-1}, and wavelength range of 4000–1400 cm^{-1}. The OMNIC Picta expert software (Thermo Fisher Scientific) was used to identify potential MPs using correlation maps, which were obtained by comparing the spectrum map of the filter with the reference spectra. To confirm the presence of MP particles, potential MP particles were observed under an optical microscope, and their IR spectra were compared with those in the library. Particles with the expected shapes and having a spectrum similarity greater than 70% were confirmed as MP particles. All of the microscopic images of the identified MPs were saved, and their size parameters (e.g., diameter and length of the cylindrical MPs, length of long and short perpendiculars at the midpoint for fragmented MPs) were recorded.

2.7. Observation of biofilm development at MP surfaces

Changes at the surfaces of the cylindrical reference MPs before and after incubation in the WWTP influent were observed using an optical microscope. Approximately 20 cylindrical reference HDPE, PP, PS, and PET particles were counted, and their images were obtained using an optical microscope. After counting, all MPs of each material were added to a 20 mL conical tube containing 5 mL of the influent. The tubes were incubated for two weeks under the same conditions specified in section 2.3. After incubation, the influent was directly filtered through a 25-mm Anodisc filter membrane with a pore size of 0.2 μm, and the MPs on the filters were observed using an optical microscope. For better observation of the MP surfaces, scanning electron microscopy (SEM) images were obtained. After the optical analysis of the Anodisc filter, it was completely dried in a desiccator. The position of reference MPs was inspected on the dried filter, after which a carbon conductive adhesive double-sided tape (width: 5 mm, thickness: 0.16 mm; Woo Yang Korea Chemical, Seoul, Republic of Korea) was lightly attached to the filter and then removed. The carbon tape with adhered MPs was fixed to the SEM mount, and the surfaces of the MPs were observed using FE-SEM with a Quanta™ 250 FEG (ThermoFisher Scientific).

2.8. Predicting and comparing the settling of MPs

The observed settling behavior of pristine MP particles can be explained by the theoretical terminal velocity of a spherical particle (u_t) in a creeping flow with a very low Reynolds number (Re). When the Re around the MP particles (Re_p) is extremely small ($Re_p \ll 1$), the settling velocity of an MP particle is estimated by Stokes' law (Eq. (1)), assuming that the acceleration in the Navier–Stokes equation is negligible, as follows:

$$u_t = \left(\frac{4d_{eq}(\rho_m - \rho_f)}{3C_D\rho_f}g\right)^{\frac{1}{2}} \quad (1)$$

where d_{eq} is the equivalent spherical diameter with the same volume as that of the particle [m], ρ_f and ρ_m are the densities of the fluid and particle [kg m^{-3}], respectively; C_D is the drag coefficient; and g is the gravitational acceleration [m s^{-2}].

In the Stokes regime where $Re_p < 0.1$, C_D is calculated as $C_D = 24/Re_p$. Moreover, d_{eq} was calculated using the measured size of the MP particles, assuming a spherical shape. As the MPs used in the experiment were cylindrical or fragmented, the equivalent diameter d_{eq} was calculated using the measured lengths. In the case of cylindrical MPs with diameters d and heights h, d_{eq} was calculated using Eq. (2):

$$d_{eq} = \left(\frac{3d^2h}{2}\right)^{\frac{1}{3}} \quad (2)$$

When the h of an MP was not measurable; it was assumed to be the same as d. In the case of fragmented MPs, d_{eq} was calculated using Eq. (3), assuming that the shape of fragmented MPs was ellipsoid.

$$d_{eq} = 2\left(a^2b\right)^{\frac{1}{3}} \quad (3)$$

where, a is the short semi-axis length and b is the long semi-axis length. Given that only 2-D images of the MPs were obtained from the experiment, the other semi-axis length of the MPs was assumed to be the same as the short semi-axis length measured in the experiment.

To compare the experimental results and predictions obtained using Stokes' law, the settling probabilities of the MPs were calculated. The u_t of the pristine MPs, calculated using d_{eq} and obtained from Eq. (1), was compared with the upward flow velocity at a radial distance r from the center of the flow cross-section (u_r) in the test apparatus. When u_t was greater than u_r, the MP was considered to be sedimented. The Re of the flow in the test column ($Re = Ud_c/\nu$, where d_c is the diameter of the glass cylinder for the experiment and U is the average stream velocity) ranged between 3.25 and 9.75 and corresponds to laminar flow. This allowed the prediction of u_r, assuming a parabolic velocity profile, as follows (White, 2016):

$$u_r = U_0\left[1 - \left(\frac{r}{R}\right)^2\right] \quad (4)$$

where, R is the radius of the cylinder and U_0 is the maximum flow velocity at the centerline $r = 0$. Moreover, a no-slip boundary condition ($u_r = 0$ at the wall ($r = R$)) was assumed.

The test system was run at a steady flow, and u_r was assumed to be constant at every height. The cross-sectional area of the cylinder where $u_t > u_r$ was calculated for particles with d_{eq}. This allowed the probability of sedimentation of the MPs ($P_{\text{sedimented}}$) to be calculated as follows:

$$P_{\text{sedimented}} = \frac{crossectional\ area\ where\ u_t > u_r}{total\ cross - sectional\ area} \quad (5)$$

3. Results and discussion

3.1. Characterization of standard MPs

Before the settling experiments, the size and shape of the reference MP particles were determined. Table S1 summarizes the average diameter and length of the cylindrical reference MPs, including the standard deviation and measured number of MPs. The average diameter and length of the cylindrical MPs were 79.44–130.98 μm and 97.91–128.35 μm, respectively. Given that the shapes of the fragmented reference MPs were irregular, they were assumed to be ellipsoid. The equivalent diameter (d_{eq}) of a sphere with the same volume was calculated from the long and short axes of an ellipsoid. The average d_{eq} was 31.85 ± 10.51 μm (n = 223) for PS and 58.21 ± 24.52 μm (n = 166) for PET, which were smaller than those of the cylindrical reference MPs. The size distribution of each reference MP is described in Figs. S2 and S3.

SEM images of the reference MPs are presented in Figs. S4 and S5.

The shape of the cylindrical reference MPs was regular, but the fragmented reference MPs showed considerable differences in their size and shape as well as had greater surface roughness. These surface properties not only influenced the behavior of the MPs during vertical transport in the water, but also affected biofilm formation at the surface of the MPs and altered their sedimentation properties.

3.2. Vertical transport of MPs

3.2.1. Comparison of pristine and cultured MPs

Vertical transport of the identified MPs was divided into three groups, namely overflowed, suspended, and settled. Although the MP particles suspended in the middle region of the column did not overflow during the experiment, they were considered to overflow because their steady settling velocity was lower than the overflow velocities.

In Fig. 2, the distribution of the reference MPs in the settling column at three flow velocities is presented by comparing the pristine and incubated MPs. For HDPE and PP (Fig. 2a and b), it was expected that all pristine reference MPs would overflow because their material densities were lower than that of the wastewater influent (1.008 g cm^{-3}). However, approximately 10% of the HDPE and PP were isolated in the settled region at the slowest overflow velocity (0.15 mm s^{-1}), and they did not settle at higher overflow velocities. As the MPs were injected in the direction opposite to the flow of the test system using a syringe with a long stainless tube (Fig. 1), the initial sticking to the bottom surfaces of the column at the lowest overflow velocity could have prohibited buoyant transport. Interestingly, culturing HDPE and PP particles in the wastewater influent consistently resulted in an increased settled fraction at all three overflow velocities. This could be due to the growth of particles via aggregation and/or an increase in the particle density.

The settled fraction of the cylindrical reference PS and PET particles was significantly greater than those of the HDPE and PP particles at all three overflow velocities (Fig. 2c and d). This was because particle densities of PS and PET were much greater than those of the wastewater influent. Similarly, incubation with PS and PET enhanced particle settling under all the experimental conditions. The proportion of settled MPs decreased with an increasing overflow velocity. This tendency was more apparent for cylindrical PS than for cylindrical PET. Moreover, incubation increased the fractions of settled PS and PET by factors of 2.4–5.15 and 1.4–3.0, respectively. The greater effects of incubation on PS might be explained by the difference in the densities of PS (1.04 g cm^{-3}) and PET (1.37 g cm^{-3}).

Contrary to the general theory that settling velocity increases with an increase in the hydrodynamic diameter of a particle (Khatmullina and Isachenko, 2017; Stokes, 1851; Waldschläger and Schüttrumpf, 2019), the proportion of settled pristine fragmented PS particles was almost

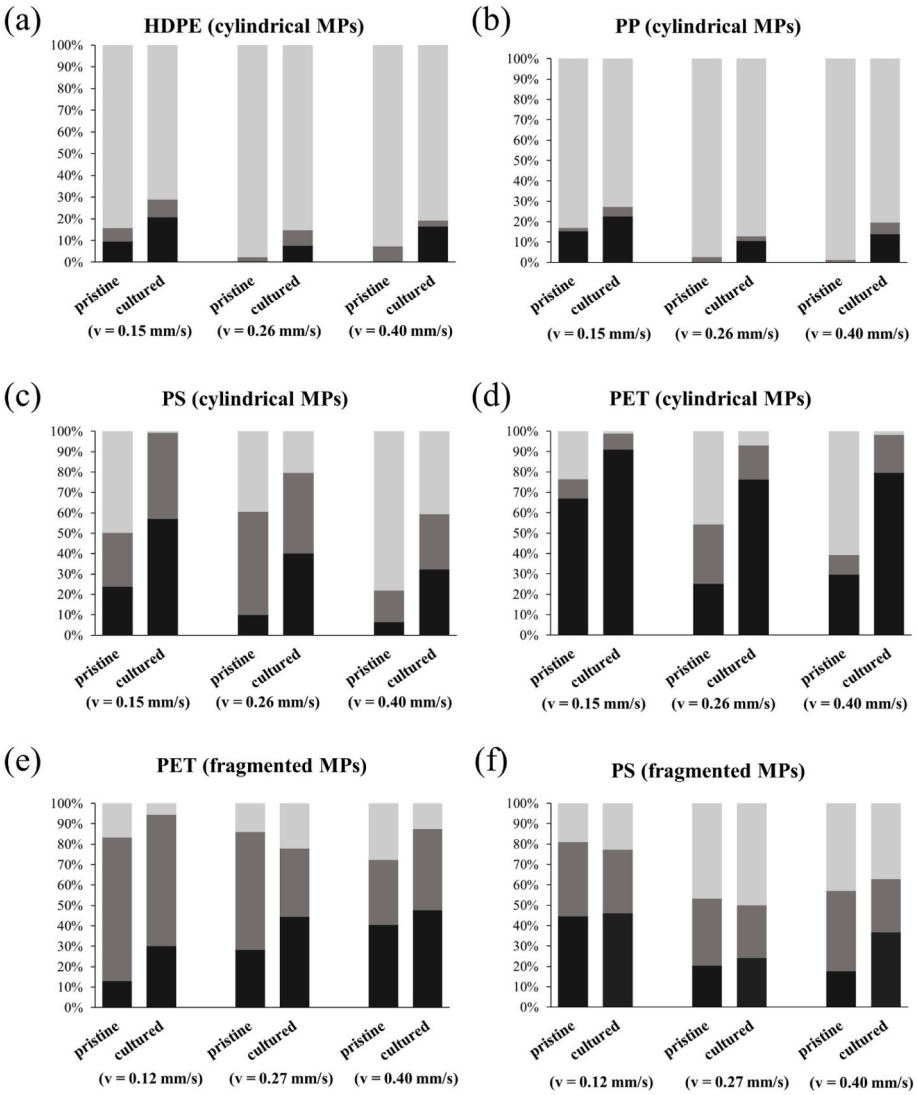

Fig. 2. Percentage of reference MPs sedimented, suspended, and overflowed in the test apparatus for (a) cylindrical HDPE, (b) cylindrical PP, (c) cylindrical PS, (d) cylindrical PET, (e) fragmented PS, and (f) fragmented PET at three flow velocities. Pristine and cultured reference MPs in the wastewater influent are compared.

twice that of the cylindrical PS particles (Fig. 2c and e). The faster settling could be explained by the fact that pristine fragmented PS particles aggregated easily after they were added to the settling apparatus, owing to their irregular shape and larger specific surface area that favored entanglement. Although the wastewater influent was filtered through a stainless filter with a 20 μm pore size, suspended organic and inorganic particles of smaller sizes remained. As fragmented PS particles are much smaller than cylindrical PS particles, the aggregation of fragmented PS with suspended particles may significantly alter their particle size and density. As opposed to the cylindrical PS particles, incubation of the fragmented PS did not increase the settling behavior (Fig. 2c and e), possibly because the fragmented PS sufficiently aggregated in the test apparatus without incubation, whereas the cylindrical PS did not.

The smaller particle size of the fragmented PET partly explains the smaller sediment fraction (Fig. 2f). However, an increase in the sediment fraction of the fragmented PET with an increase in the overflow velocity was not consistent with other studies. It was found that large negative charges on MP surfaces increase the diversity of MPs during their incubation in freshwater (Ramsperger et al., 2020), which might be related to the complex settling behavior of fragment PET particles after biofilm formation, as the surface charge of PET is known to be very negative. Further investigation is required to understand if the interaction between fragmented PET particles and the glass wall affected the results of the experiment.

Murphy et al. (2016) investigated the effects of polymer composition in liquid (influent and effluent) and solid (grit, grease, and sludge cake (SC)) fractions on the number of MPs during four stages of the treatment processes in a large secondary WWTP in River Clyde, Glasgow, using FT-IR imaging. They isolated HDPE and PP particles in the SC of a primary clarifier and concluded that the settling fractions of HDPE and PP were low. However, in their study, most of the HDPE and PP overflowed, which is consistent with the low settling of HDPE and PP. After the primary treatment, the percentages of PS and PET in the liquid fraction decreased from 17.2% to 5.9% and 12.6%–2.9%, respectively. This was consistent with the experimental results of this study that concluded that 20–45% of PS and 30–90% of PET incubated in the WWTP influent had settled. The size range of the MPs used in Murphy et al. (2016) was 598–1618 μm, which is larger than the size range used in our study (31.85–130.98 μm). In our study, the removal efficiency of MP particles was estimated by calculating the settled mass fraction of MPs. The measured density and size of the MP particles recorded from the image analysis during the FT-IR analysis was used for estimating the mass of the MP particles (examples of spectra and microscope images are in Fig. S6). The fragmented reference MPs were assumed to be ellipsoids. The removal rates of HDPE, PP, PS, and PET with sizes of approximately 150 μm were estimated as 6.3 ± 1.9%, 15.0 ± 0.9%, 60.8 ± 18.0%, and 86.2 ± 9.1%, respectively, in a typical primary clarifier with a retention time of 2 h in the WWTPs. Additionally, the smaller (20–100 μm) and irregularly shaped MP particles were predicted to be more difficult to remove by settling than the cylindrical particles of similar sizes, with removal rates of 19.1 ± 0.3% and 48.5 ± 3.6% for PS and PET, respectively.

As previously discussed, the settling velocity of the reference MP particles significantly increased with increasing particle size and density. This general tendency was more apparent for the cylindrical reference MPs than for the fragmented reference MPs and coincides with previous studies that used larger MP particles (diameter: 0.4–5 mm). The tested settling velocities in this study (0.15–0.40 mm s^{-1}) were considerably smaller than those in previous studies using larger particles (0.3–11 cm s^{-1}) (Waldschläger and Schüttrumpf, 2019; Semcesen and Wells, 2021). This indicates that it is more difficult to remove smaller MPs by gravitational settling in a typical WWTP, and partly supports previous investigations in which MPs in WWTP effluents were generally smaller than those in influents (Dris et al., 2015; Simon et al., 2018; Talvitie et al., 2017). Because sedimentation is the most important removal mechanism for MPs, further research on how the aggregation of MPs can be enhanced to improve the removal efficiency and, thus, reduce the load of MPs in public waterways should be conducted. The increase in the settling velocity of the MPs after incubation in the wastewater influent supports the observation of light-density MPs in wastewater sludge (Mahon et al., 2017; Mintenig et al., 2017; Murphy et al., 2016) and sediments of freshwater systems (Koutnik et al., 2021). Given that MPs in water are largely fragmented (Di and Wang, 2018; Free et al., 2014; Park et al., 2020; Sol et al., 2020), further studies on the effects of shape on aggregation and entanglement in the presence of naturally occurring suspended particles under various environmental conditions are required.

3.2.2. Comparing the settling of MPs with theoretical predictions

To compare the experimental results and predictions obtained using Stokes' law, the settling probabilities of the MPs were calculated using Eq. (5). The theoretical probability of sedimentation was compared with the experimental data for the reference PS and PET particles that had densities greater than that of wastewater (Fig. 3 and S7). The settled fraction predicted by the Stokes equation was significantly greater than that observed under most experimental conditions. However, in the case of the fragmented reference PS, the measured settled fractions were marginally higher than the predicted fraction. Although there was a significant difference between the predicted and measured settled fractions, the measured settled fraction increased as the size of the particles of all the reference MPs increased; this was demonstrated in the modeling results (Fig. 3). The comparisons between the predicted and measured settled fractions of the reference PS and PET at other flow velocities (0.12 and 0.40 mm s^{-1}) were similar to those at a flow velocity of 0.27 mm s^{-1}.

The difference between the experimental results and theoretical predictions could be due to (1) the introduction of reference MP particles closer to the center of the flow cross-section (the model assumed a homogeneous distribution in the flow cross-section) and (2) larger drag coefficients of the reference MP particles. If all the particles were introduced at the center of the flow cross-section, the calculated critical d_{eq} for the cylindrical and fragmented reference PET with settling velocities equal to U_0 were 91 and 87 μm, respectively. This explains the lower percentage of settled PET particles in the experiment. The calculated d_{eq} was 176 and 250 μm for the cylindrical and fragmented PS, respectively. This was outside the size range chosen for the experiment, thereby supporting the observation of a lower settling probability.

As the equation used for calculating the settling velocities based on Stokes' law was obtained under limited conditions, it was necessary to consider the inertia terms in the Navier–Stokes equation and particle shape factors. When correcting the drag coefficients in our data using an equation that partly considers inertia terms (Dey et al., 2019), C_D increased by a factor of up to 1.12, resulting in minor changes. When the drag coefficients were corrected using an equation for non-spherical particles (Bagheri and Bonadonna, 2016), the correction factors for C_D ranged from 1.0070 to 1.0104 for the reference PS and PET, respectively. It was concluded that the surface roughness of a particle influences C_D, although small-scale irregularities and surface vesicularities do not significantly alter the drag coefficient for irregular particles in the Stokes regime (Bagheri and Bonadonna, 2016; Hill and Power, 1956). Therefore, a higher C_D that considers inertia and shape factors would have minimal effects on the observed settling.

3.3. Changes at MP surfaces after incubation in wastewater influent

The growth of biofilm at the surface of the cylindrical reference MPs after incubation in the wastewater influent was observed using optical microscopy and SEM (Fig. 4). The surfaces of all types of the MPs were partially covered by a green layer, indicating the formation of biofilm. As the biofilm was not sufficiently developed to quantitatively estimate the growth of particle size, changes in the density of individual MPs were not predictable. In the SEM images, it was apparent that the MP

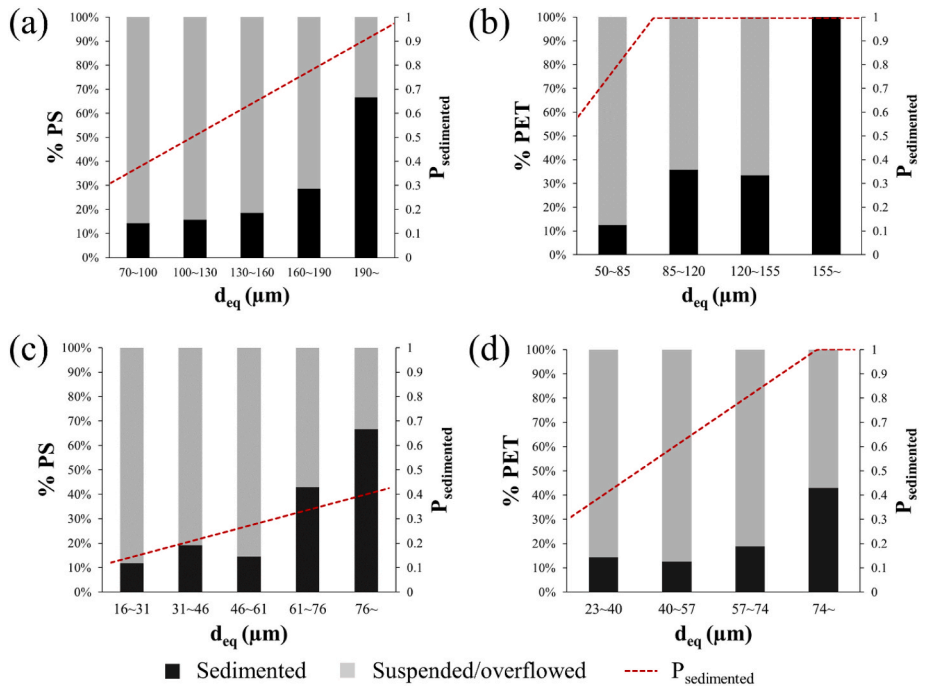

Fig. 3. Percentage of sedimented and suspended/overflowed pristine reference MPs in wastewater influent with theoretically predicted sedimentation probability at a flow velocity of 0.27 mm s^{-1} for (a) cylindrical PS, (b) cylindrical PET, (c) fragmented PS, and (d) fragmented PET.

surfaces were colonized by various species. Compared with the surface of pristine MPs (Fig. S4), the surfaces of MPs incubated in the wastewater influent were rougher and more heterogeneous. Such surface changes may affect sedimentation properties by altering the affinity between MPs or other particles in the wastewater influent. In addition, biofilm makes the surface of a particle stickier, thereby allowing further aggregation and settling of MP particles (Fazey and Ryan, 2016; Long et al., 2015). This hypothesis is strongly supported by the observation that a significant percentage of cultured HDPE and PP particles were sedimented, whereas the pristine reference MPs were not. This notable increase in the settling velocity of light-density MPs is consistent with previous studies, which demonstrated that the surfaces of MPs become more hydrophilic (Lobelle and Cunliffe, 2011) and denser with biofilm formation (Kaiser et al., 2017; Semcesen and Wells, 2021; Wu et al., 2020).

3.4. Implications of the study

The vertical settling properties of MPs with different densities provide insights into the fate and transport of MPs in WWTPs and freshwater systems, where turbulence has a limited impact. It has been concluded that WWTPs are a major source of MPs in aquatic and terrestrial environments as they discharge effluents and sludge (Hu et al., 2022). The removal of MPs is generally achieved by particle settling in primary and secondary clarifiers (Carr et al., 2016; Dris et al., 2015; Gies et al., 2018; Long et al., 2022; Talvitie et al., 2015; Yang et al., 2019). In static freshwater bodies, such as lakes, ponds, and reservoirs, MPs can settle in bottom sediments and can be stored for long periods (Di and Wang, 2018; Hu et al., 2018; Sruthy and Ramasamy, 2017; Welden and Lusher, 2020). The settling of reference MPs before and after biofilm development in a laboratory setting revealed that the sedimentation of MPs was greatly enhanced by aggregation with other suspended particles in water, supporting previous results that low-density MPs are widely detected in freshwater sediment samples (Di and Wang, 2018; Xiong et al., 2018). The range of the estimated settling velocity (0.1–0.4 mm s^{-1}) of MP materials of different sizes and their sedimentation efficiencies in a wastewater clarifier (6.33–86.20% by mass) could be used to predict the removal of MPs entering a WWTP based on operational parameters, such as the overflow velocity and mixed liquor suspended solid concentration. This could reduce the effort required for isolating and identifying MPs in WWTPs.

The settling behavior of fragmented MP particles is more complex than that of regularly shaped particles. Most of the secondary MPs detected in environmental samples are fragments or fibers. Thus, further studies are required to understand their aggregation and/or entanglement in the presence of other naturally occurring particles. It is also necessary to extend the particle dynamics of MPs to 3-D to evaluate the transport of MPs in non-static waterbodies.

4. Conclusions

Sedimentation of reference MPs under the low *Re* regime was significantly affected by aggregation of MPs with other suspended particles in wastewater influent. Biofilm formation at MP surfaces favored the growth of particles and increased the sedimented fraction by 0–16% for light MP particles (HDPE and PP) and by a factor of 1.03–5.15 for denser MP particles (PS and PET). The shape of the MPs was also an important factor affecting the floating or sinking behavior, and more complex behavior is expected for irregularly shaped MPs. In general, the settling of MPs observed during the laboratory tests coincided with the theoretical predictions obtained using Stokes' law, although the observed settling of pristine PS was different from that of PET. As vertical transport of MPs is important for evaluating their removal from wastewater clarifiers and sedimentation in waterbodies, the experimental findings of this study can be used to develop models that predict removal efficiencies in WWTPs and to estimate the sinking of MPs to bottom sediments.

Author statement

So-Yong Lee: Conceptualization, Methodology, Formal analysis, Investigation, Writing-Original Draft, Visualization, Jiyul Ahn: Investigation, Jin-Woo Kim: Investigation, Jung-Hwan Kwon: Conceptualization, Writing-Review& Edition, Supervision.

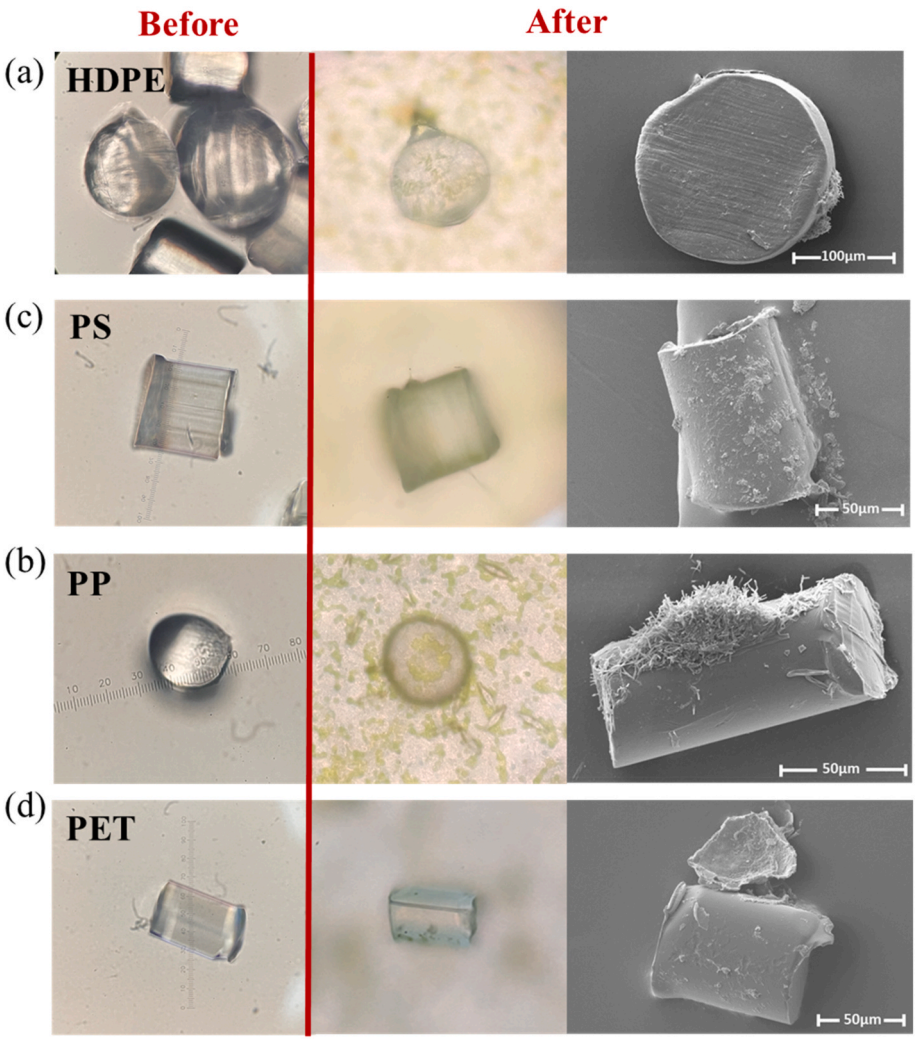

Fig. 4. Microscope images of cylindrical standard MPs before (left) and after (middle) incubation in wastewater influent for two weeks, and sample images of SEM analysis (right) of cylindrical standard MPs after culturing: (a) HDPE, (b) PP, (c) PS, and (d) PET. MPs in the microscope images were traced before and after incubation, but plastics in the SEM images were not.

Declaration of competing interest

The authors declare that they have no known competing financial interests or personal relationships that could have appeared to influence the work reported in this paper.

Data availability

Data will be made available on request.

Acknowledgments

This work was supported by the National Research Foundation of Korea (NRF) grants funded by the Korean government (MEST) [grant number 2020R1A2C2009244]. The authors would like to acknowledge Dr. Jaehak Jeong at Texas A&M University for providing valuable insights into the settling processes.

Appendix A. Supplementary data

Supplementary data to this article can be found online at https://doi.org/10.1016/j.envpol.2022.119909.

References

Adyel, T.M., 2020. Accumulation of plastic waste during COVID-19. Science 369, 1314–1315. https://doi.org/10.1126/science.abd9925.

Alimi, O.S., Farner Budarz, J., Hernandez, L.M., Tufenkji, N., 2018. Microplastics and nanoplastics in aquatic environments: aggregation, deposition, and enhanced contaminant transport. Environ. Sci. Technol. 52, 1704–1724. https://doi.org/10.1021/acs.est.7b05559.

An, D., Na, J., Song, J., Jung, J., 2021. Size-dependent chronic toxicity of fragmented polyethylene microplastics to *Daphnia magna*. Chemosphere 271, 129591. https://doi.org/10.1016/j.chemosphere.2021.129591.

Andrady, A.L., 2005. Common Plastics Materials. Plastics and the Environment. John Wiley & Sons Inc.

Atc, Europe, 2021. Document 141 - Definition of Microplastic within EU REACH Restriction.

Bagheri, G., Bonadonna, C., 2016. On the drag of freely falling non-spherical particles. Powder Technol. 301, 526–544. https://doi.org/10.1016/j.powtec.2016.06.015.

Baldwin, A.K., Corsi, S.R., Mason, S.A., 2016. Plastic debris in 29 Great Lakes tributaries: relations to watershed attributes and hydrology. Environ. Sci. Technol. 50, 10377–10385. https://doi.org/10.1021/acs.est.6b02917.

Beuth Plastics - methods for determining the density of noncellular plastics - Part 1: immersion method, liquid pyknometer method and titration method (ISO 1183−1: 2012). Beuth, 1183−1181.

Bhagat, J., Nishimura, N., Shimada, Y., 2021. Toxicological interactions of microplastics/nanoplastics and environmental contaminants: current knowledge and future perspectives. J. Hazard Mater. 405, 123913 https://doi.org/10.1016/j.jhazmat.2020.123913.

Borrelle, S.B., Ringma, J., Law, K.L., Monnahan, C.C., Lebreton, L., McGivern, A., Murphy, E., Jambeck, J., Leonard, G.H., Hilleary, M.A., Eriksen, M., Possingham, H. P., de Frond, H., Gerber, L.R., Polidoro, B., Tahir, A., Bernard, M., Mallos, N., Barnes, M., Rochman, C.M., 2020. Predicted growth in plastic waste exceeds efforts

to mitigate plastic pollution. Science 369, 1515–1518. https://doi.org/10.1126/science.aba3656.
Carr, S.A., Liu, J., Tesoro, A.G., 2016. Transport and fate of microplastic particles in wastewater treatment plants. Water Res. 91, 174–182. https://doi.org/10.1016/j.watres.2016.01.002.
Cózar, A., Echevarría, F., González-Gordillo, J.I., Irigoien, X., Úbeda, B., Hernández-León, S., Palma, A.T., Navarro, S., García-de-Lomas, J., Ruiz, A., Fernández-de-Puelles, M.L., Duarte, C.M., 2014. Plastic debris in the open ocean. Proc. Natl. Acad. Sci. U. S. A. 111 (28), 10239–10244. https://doi.org/10.1073/pnas.1314705111.
Deowan, S.A., Bouhadjar, S.I., Hoinkis, J., 2015. 5 - membrane bioreactors for water treatment. In: Basile, A., Cassano, A., Rastogi, N.K. (Eds.), Advances in Membrane Technologies for Water Treatment. Woodhead Publishing., pp. 155–184. https://doi.org/10.1016/B978-1-78242-121-4.00005-8
Dey, S., Zeeshan Ali, S., Padhi, E., 2019. Terminal fall velocity: the legacy of Stokes from the perspective of fluvial hydraulics. Proc. Math. Phys. Eng. Sci. 47, 20190277 https://doi.org/10.1098/rspa.2019.0277.
Di, M., Wang, J., 2018. Microplastics in surface waters and sediments of the three gorges reservoir, China. Sci. Total Environ. 616–617, 1620–1627. https://doi.org/10.1016/j.scitotenv.2017.10.150.
Dris, R., Gasperi, J., Rocher, V., Saad, M., Renault, N., Tassin, B., 2015. Microplastic contamination in an urban area: a case study in Greater Paris. Environ. Chem. 12, 592–599. https://doi.org/10.1071/en14167.
Eo, S., Hong, S.H., Song, Y.K., Han, G.M., Shim, W.J., 2019. Spatiotemporal distribution and annual load of microplastics in the Nakdong River, South Korea. Water Res. 160, 228–237. https://doi.org/10.1016/j.watres.2019.05.053.
Fazey, F.M., Ryan, P.G., 2016. Biofouling on buoyant marine plastics: an experimental study into the effect of size on surface longevity. Environ. Pollut. 210, 354–360. https://doi.org/10.1016/j.envpol.2016.01.026.
Fischer, E.K., Paglialonga, L., Czech, E., Tamminga, M., 2016. Microplastic pollution in lakes and lake shoreline sediments - a case study on Lake Bolsena and Lake Chiusi (central Italy). Environ. Pollut. 213, 648–657. https://doi.org/10.1016/j.envpol.2016.03.012.
Free, C.M., Jensen, O.P., Mason, S.A., Eriksen, M., Williamson, N.J., Boldgiv, B., 2014. High-levels of microplastic pollution in a large, remote, mountain lake. Mar. Pollut. Bull. 85, 156–163. https://doi.org/10.1016/j.marpolbul.2014.06.001.
Ge, J., Li, H., Liu, P., Zhang, Z., Ouyang, Z., Guo, X., 2021. Review of the toxic effect of microplastics on terrestrial and aquatic plants. Sci. Total Environ. 791, 148333 https://doi.org/10.1016/j.scitotenv.2021.148333.
Gies, E.A., LeNoble, J.L., Noel, M., Etemadifar, A., Bishay, F., Hall, E.R., Ross, P.S., 2018. Retention of microplastics in a major secondary wastewater treatment plant in Vancouver, Canada. Mar. Pollut. Bull. 133, 553–561. https://doi.org/10.1016/j.marpolbul.2018.06.006.
Hill, R.P., Power, G., 1956. Extremum principles for slow viscous flow and the approximate calculation of drag. Q. J. Mech. Appl. Math. 9 (3), 313–319.
Horton, A.A., Walton, A., Spurgeon, D.J., Lahive, E., Svendsen, C., 2017. Microplastics in freshwater and terrestrial environments: evaluating the current understanding to identify the knowledge gaps and future research priorities. Sci. Total Environ. 586, 127–141. https://doi.org/10.1016/j.scitotenv.2017.01.190.
Hu, K., Yang, Y., Zuo, J., Tian, W., Wang, Y., Duan, X., Wang, S., 2022. Emerging microplastics in the environment: properties, distributions, and impacts. Chemosphere 297, 134118. https://doi.org/10.1016/j.chemosphere.2022.134118.
Hu, L., Chernick, M., Hinton, D.E., Shi, H., 2018. Microplastics in small waterbodies and tadpoles from yangtze river delta, China. Environ. Sci. Technol. 52, 8885–8893. https://doi.org/10.1021/acs.est.8b02279.
Iyare, P.U., Ouki, S.K., Bond, T., 2020. Microplastics removal in wastewater treatment plants: a critical review. Environ. Sci.: Water Res. Technol. 6, 2664–2675. https://doi.org/10.1039/d0ew00397b.
Kaiser, D., Kowalski, N., Waniek, J.J., 2017. Effects of biofouling on the sinking behavior of microplastics. Environ. Res. Lett. 12, 124003 https://doi.org/10.1088/1748-9326/aa8e8b.
Kang, H.J., Lee, S.Y., Kwon, J.H., 2016. Physico-chemical properties and toxicity of alkylated polycyclic aromatic hydrocarbons. J. Hazard Mater. 312, 200–207. https://doi.org/10.1016/j.jhazmat.2016.03.051.
Karabelas, A.J., Plakas, K.V., Sarasidis, V.C., 2018. Chapter 9 - how far are we from large-scale PMR applications? In: Basile, A., Mozia, S., Molinari, R. (Eds.), Current Trends and Future Developments on (Bio-) Membranes. Elsevier, pp. 233–295. https://doi.org/10.1016/B978-0-12-813549-5.00009-8.
Khatmullina, L., Isachenko, I., 2017. Settling velocity of microplastic particles of regular shapes. Mar. Pollut. Bull. 114, 871–880. https://doi.org/10.1016/j.marpolbul.2016.11.024.
Kokalj, A.J., Kunej, U., Skalar, T., 2018. Screening study of four environmentally relevant microplastic pollutants: uptake and effects on *Daphnia magna* and *Artemia franciscana*. Chemosphere 208, 522–529. https://doi.org/10.1016/j.chemosphere.2018.05.172.
Koutnik, V.S., Leonard, J., Alkidim, S., DePrima, F.J., Ravi, S., Hoek, E.M.V., Mohanty, S. K., 2021. Distribution of microplastics in soil and freshwater environments: global analysis and framework for transport modeling. Environ. Pollut. 274, 116552 https://doi.org/10.1016/j.envpol.2021.116552.
Lahens, L., Strady, E., Kieu-Le, T.C., Dris, R., Boukerma, K., Rinnert, E., Gasperi, J., Tassin, B., 2018. Macroplastic and microplastic contamination assessment of a tropical river (Saigon River, Vietnam) transversed by a developing megacity. Environ. Pollut. 236, 661–671. https://doi.org/10.1016/j.envpol.2018.02.005.
Law, K.L.T., Thompson, R.C., 2014. Microplastics in the seas Concern is rising about widespread contamination of the marine environment by microplastics. Science 345, 144–145. https://doi.org/10.1126/science.1254065.
Lobelle, D., Cunliffe, M., 2011. Early microbial biofilm formation on marine plastic debris. Mar. Pollut. Bull. 62, 197–200. https://doi.org/10.1016/j.marpolbul.2010.10.013.
Long, M., Moriceau, B., Gallinari, M., Lambert, C., Huvet, A., Raffray, J., Soudant, P., 2015. Interactions between microplastics and phytoplankton aggregates: impact on their respective fates. Mar. Chem. 175, 39–46. https://doi.org/10.1016/j.marchem.2015.04.003.
Long, Y., Zhou, Z., Yin, L., Wen, X., Xiao, R., Du, L., Zhu, L., Liu, R., Xu, Q., Li, H., Nan, R., Yan, S., 2022. Microplastics removal and characteristics of constructed wetlands WWTPs in rural area of Changsha, China: a different situation from urban WWTPs. Sci. Total Environ. 811, 152352 https://doi.org/10.1016/j.scitotenv.2021.152352.
Ma, H., Pu, S., Liu, S., Bai, Y., Mandal, S., Xing, B., 2020. Microplastics in aquatic environments: toxicity to trigger ecological consequences. Environ. Pollut. 261, 114089 https://doi.org/10.1016/j.envpol.2020.114089.
Mahon, A.M., O'Connell, B., Healy, M.G., O'Connor, I., Officer, R., Nash, R., Morrison, L., 2017. Microplastics in sewage sludge: effects of treatment. Environ. Sci. Technol. 51, 810–818. https://doi.org/10.1021/acs.est.6b04048.
McCormick, A., Hoellein, T.J., Mason, S.A., Schluep, J., Kelly, J.J., 2014. Microplastic is an abundant and distinct microbial habitat in an urban river. Environ. Sci. Technol. 48, 11863–11871. https://doi.org/10.1021/es503610r.
Meijer, L.J.J., van Emmerik, T., van der Ent, R., Schmidt, C., Lebreton, L., 2021. More than 1000 rivers account for 80% of global riverine plastic emissions into the ocean. Sci. Adv. 7, 1–13. https://doi.org/10.1126/sciadv.aaz5803.
Miao, L., Wang, P., Hou, J., Yao, Y., Liu, Z., Liu, S., Li, T., 2019. Distinct community structure and microbial functions of biofilms colonizing microplastics. Sci. Total Environ. 650 (Pt 2), 2395–2402. https://doi.org/10.1016/j.scitotenv.2018.09.378.
Michels, J., Stippkugel, A., Lenz, M., Wirtz, K., Engel, A., 2018. Rapid aggregation of biofilm-covered microplastics with marine biogenic particles. Proc. Biol. Sci. 285, 20181203 https://doi.org/10.1098/rspb.2018.1203.
Mintenig, S.M., Int-Veen, I., Loder, M.G.J., Primpke, S., Gerdts, G., 2017. Identification of microplastic in effluents of waste water treatment plants using focal plane array-based micro-Fourier-transform infrared imaging. Water Res. 108, 365–372. https://doi.org/10.1016/j.watres.2016.11.015.
Murphy, F., Ewins, C., Carbonnier, F., Quinn, B., 2016. Wastewater treatment works (WwTW) as a source of microplastics in the aquatic environment. Environ. Sci. Technol. 50, 5800–5808. https://doi.org/10.1021/acs.est.5b05416.
OECD, 2011. Test No. 201: Freshwater Alga and Cyanobacteria, Growth Inhibition Test. OECD Guidelines for the Testing of Chemicals, Section 2. OECD Publishing, Paris, France.
Park, H.J., Oh, M.J., Kim, P.G., Kim, G., Jeong, D.H., Ju, B.K., Lee, W.S., Chung, H.M., Kang, H.J., Kwon, J.H., 2020. National reconnaissance survey of microplastics in municipal wastewater treatment plants in Korea. Environ. Sci. Technol. 54, 1503–1512. https://doi.org/10.1021/acs.est.9b04929.
Plastics Europe & EPRO, 2021. Plastics - the Facts 2021: an Analysis of European Plastics Production, Demand and Waste Data 34. https://plasticseurope.org/knowledge-hub/plastics-the-facts-2021/.
Ramsperger, A.F.R.M., Stellwag, A.C., Caspari, A., Fery, A., Lueders, T., Kress, H., Löder, M.G.J., Laforsch, C., 2020. Structural diversity in early-stage biofilm formation on microplastics depends on environmental medium and polymer properties. Water 12, 3216. https://doi.org/10.3390/w12113216.
Rochman, C.M., 2018. Microplastics research—from sink to source. Science 360, 28–29. https://doi.org/10.1126/science.aar7734.
Semcesen, P.O., Wells, M.G., 2021. Biofilm growth on buoyant microplastics leads to changes in settling rates: implications for microplastic retention in the Great Lakes. Mar. Pollut. Bull. 170, 112573 https://doi.org/10.1016/j.marpolbul.2021.112573.
Simon, M., van Alst, N., Vollertsen, J., 2018. Quantification of microplastic mass and removal rates at wastewater treatment plants applying Focal Plane Array (FPA)-based Fourier Transform Infrared (FT-IR) imaging. Water Res. 142, 1–9. https://doi.org/10.1016/j.watres.2018.05.019.
Sol, D., Laca, A., Laca, A., Díaz, M., 2020. Approaching the environmental problem of microplastics: importance of WWTP treatments. Sci. Total Environ. 740, 140016 https://doi.org/10.1016/j.scitotenv.2020.140016.
Sruthy, S., Ramasamy, E.V., 2017. Microplastic pollution in Vembanad Lake, Kerala, India: the first report of microplastics in lake and estuarine sediments in India. Environ. Pollut. 222, 315–322. https://doi.org/10.1016/j.envpol.2016.12.038.
Stokes, G.G., 1851. On the Effect of the Internal Friction of Fluids on the Motion of Pendulum, vol. 9. Pitt. Press, p. 1.
Su, L., Xue, Y., Li, L., Yang, D., Kolandhasamy, P., Li, D., Shi, H., 2016. Microplastics in taihu lake, China. Environ. Pollut. 216, 711–719. https://doi.org/10.1016/j.envpol.2016.06.036.
Talvitie, J., Heinonen, M., Pääkkönen, J.P., Vahtera, E., Mikola, A., Setälä, O., Vahala, R., 2015. Do wastewater treatment plants act as a potential point source of microplastics? Preliminary study in the coastal Gulf of Finland, Baltic Sea. Water Sci. Technol. 72, 1495–1504. https://doi.org/10.2166/wst.2015.360.
Talvitie, J., Mikola, A., Koistinen, A., Setälä, O., 2017. Solutions to microplastic pollution - removal of microplastics from wastewater effluent with advanced wastewater treatment technologies. Water Res. 123, 401–407. https://doi.org/10.1016/j.watres.2017.07.005.
Tang, K.H.D., Hadibarata, T., 2021. Microplastics removal through water treatment plants: its feasibility, efficiency, future prospects and enhancement by proper waste management. Environ. Chall. 5, 100264 https://doi.org/10.1016/j.envc.2021.100264.
Thompson, R.C., Olsen, Y., Mitchell, R.P., Anthony, D., Rowland, S.J., John, A.W.G., McGonigle, D., Russell, A.E., 2004. Lost at sea: where is all the plastic? Science 304 (5672). https://doi.org/10.1126/science.1094559, 838-838.

van Sebille, E., Wilcox, C., Lebreton, L., Maximenko, N., Hardesty, B.D., van Franeker, J. A., Eriksen, M., Siegel, D., Galgani, F., Law, K.L., 2015. A global inventory of small floating plastic debris. Environ. Res. Lett. 10, 124006 https://doi.org/10.1088/1748-9326/10/12/124006.

Waldschläger, K., Schüttrumpf, H., 2019. Effects of particle properties on the settling and rise velocities of microplastics in freshwater under laboratory conditions. Environ. Sci. Technol. 53, 1958–1966. https://doi.org/10.1021/acs.est.8b06794.

Welden, N.A., Lusher, A., 2020. Chapter 9 - microplastics: from origin to impacts. In: Letcher, T.M. (Ed.), Microplastics: from Origin to Impacts, Plastic Waste and Recycling. Academic Press, pp. 223–249. https://doi.org/10.1016/B978-0-12-817880-5.00009-8.

White, F.M., 2016. Fluid Mechnics, eighth ed. McGraw-Hill Education, New York.

Wong, J.K.H., Lee, K.K., Tang, K.H.D., Yap, P.S., 2020. Microplastics in the freshwater and terrestrial environments: prevalence, fates, impacts and sustainable solutions. Sci. Total Environ. 719, 137512 https://doi.org/10.1016/j.scitotenv.2020.137512.

Wu, N., Zhang, Y., Li, W., Wang, J., Zhang, X., He, J., Li, J., Ma, Y., Niu, Z., 2020. Co-effects of biofouling and inorganic matters increased the density of environmental microplastics in the sediments of Bohai Bay coast. Sci. Total Environ. 717, 134431 https://doi.org/10.1016/j.scitotenv.2019.134431.

Xiong, X., Zhang, K., Chen, X., Shi, H., Luo, Z., Wu, C., 2018. Sources and distribution of microplastics in China's largest inland lake - qinghai Lake. Environ. Pollut. 235, 899–906. https://doi.org/10.1016/j.envpol.2017.12.081.

Yang, L., Li, K., Cui, S., Kang, Y., An, L., Lei, K., 2019. Removal of microplastics in municipal sewage from China's largest water reclamation plant. Water Res. 155, 175–181. https://doi.org/10.1016/j.watres.2019.02.046.

Ziajahromi, S., Kumar, A., Neale, P.A., Leusch, F.D.L., 2018. Environmentally relevant concentrations of polyethylene microplastics negatively impact the survival, growth and emergence of sediment-dwelling invertebrates. Environ. Pollut. 236, 425–431. https://doi.org/10.1016/j.envpol.2018.01.094.